# NACA

### RESEARCH MEMORANDUM

PRELIMINARY FREE-FLIGHT STUDY OF THE DRAG AND STABILITY

OF A SERIES OF SHORT-SPAN MISSILES

AT MACH NUMBERS FROM 0.9 TO 1.3

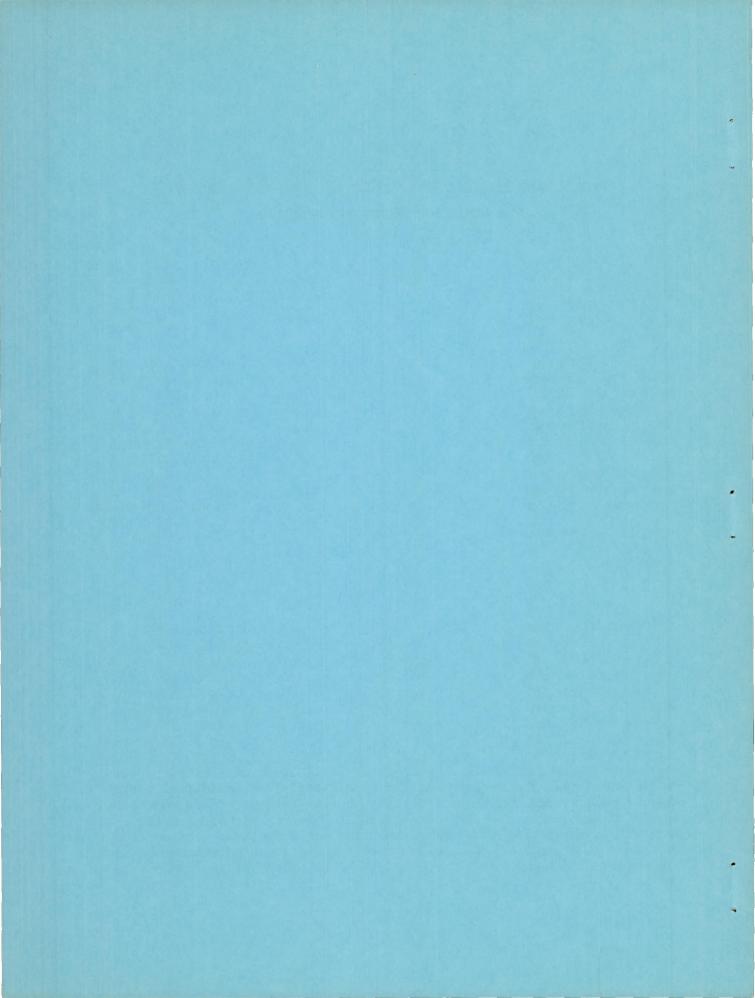
By James Rudyard Hall

Langley Aeronautical Laboratory
Langley Field, Va.

### NATIONAL ADVISORY COMMITTEE FOR AERONAUTICS

WASHINGTON

February 8, 1956
Declassified October 14, 1957



#### NATIONAL ADVISORY COMMITTEE FOR AERONAUTICS

#### RESEARCH MEMORANDUM

## PRELIMINARY FREE-FLIGHT STUDY OF THE DRAG AND STABILITY OF A SERIES OF SHORT-SPAN MISSILES AT MACH NUMBERS FROM 0.9 TO 1.3

By James Rudyard Hall

#### SUMMARY

A preliminary free-flight study has been made of the drag and stability of a series of short-span missile configurations employing 80°, 85°, and 90° of fin leading-edge sweep. Increasing the fin sweep decreased the drag markedly. The configurations employing 80° and 85° of fin leading-edge sweep were stable with a center of gravity at 54 and 52 percent of the body length, respectively. These configurations may have been stable with even more rearward center-of-gravity locations. The configuration employing 90° of leading-edge sweep was marginally stable with the center of gravity at 43 percent of the body length. The Mach number range of the tests was from 0.9 to 1.3 and the Reynolds number range (based on model length) was from 4 x 10° to 9 x 10°.

#### INTRODUCTION

The search for higher aircraft speed has emphasized the need for internal stowage of armament due to the performance penalties often associated with externally carried armament. In particular, the mounting of missiles beneath the wings of transonic and supersonic fighter type of aircraft can produce severe drag and stability penalties. A possible method of eliminating this shortcoming is to launch the missiles from tubes carried internally much the same as submarine torpedoes. Such a technique would, of course, require minimum size tubes, and missile configurations that could be made stable by fins which could pass through the tubes. Such fins would have to be retractable or of the low aspectratio vane type. The requirement for a self-contained solid-fuel rocket motor further complicates the stability problem because of the additional weight at the rear. The Pilotless Aircraft Research Division of the National Advisory Committee for Aeronautics has undertaken a brief study of a family of configurations which meet the requirements enumerated above. The experiments were carried out utilizing the 6-inch helium gun at the

NACA RM L55J13

Langley Pilotless Aircraft Research Station at Wallops Island, Va. The Reynolds number varied from  $9 \times 10^6$  at a Mach number of 1.3 to  $4 \times 10^6$  at a Mach number of 0.9 (Reynolds number based on model length).

#### SYMBOLS

a	acceleration, ft/sec <sup>2</sup>
$C_{\mathbf{D}}$	drag coefficient, Drag qS
g	acceleration of gravity, 32.2 ft/sec <sup>2</sup>
М	Mach number
q	dynamic pressure, lb/sq ft
S	frontal area of body alone, 0.00786 sq ft
W	weight, lb
γ	flight-path angle, deg
Λ	sweep angle, deg

#### EXPERIMENTAL CONFIGURATIONS AND TECHNIQUE

Sketches of experimental configurations employed are presented in figure 1. The basic fuselage incorporated a pointed parabolic nose of fineness ratio 3, a cylindrical section of fineness ratio unity, and a parabolic afterbody of fineness ratio 2 leading into a cylindrical section of fineness ratio 3 (based on maximum diameter). The overall fineness ratio is 9. The fuselage contour is intended to be a practicable armament-missile configuration. The reduced-diameter rear section is intended to house a solid-fuel rocket motor. Space is provided for the stabilizing fins (folded or otherwise) in the annulus between the rocket-motor housing and the projected diameter of the main body. The leading edges of the fins intersect the fuselage at a distance four diameters from the nose and are swept back 80°, 85°, and 90° giving three basic configurations designated 1, 2, and 3. The 80° and 85° swept fins presumably could be constructed to telescope and so be launchable through tubes.

NACA RM L55J13

A number of models with different center-of-gravity locations were constructed of each basic configuration as shown in figure 1(a). These were used to evaluate the stability or to verify that no trim changes (indicated by drag variations) took place with movement of the center of gravity. Different models of the same configuration are designated by suffixing letters to the configuration number (for example, models 1-a and 1-b).

In addition to experiments with the above basic configurations, experiments were conducted with the following modified configurations shown in figure 1:

Configuration 4: An  $80^{\circ}$  swept-fin configuration with a fully parabolic afterbody from the rear of the cylindrical center section to the base.

Configuration 5: The nose of the 90° swept-fin configuration was rounded to a radius equal to half the maximum radius.

Configuration 6: The parabolic afterbody of the 90° swept-fin configuration was replaced by an extension of the cylindrical sting. At the same time the fins were increased in span to 1.4 inches.

Configuration 3-d: The basic 90° swept-fin configuration was launched from a special sabot at 10° angle of attack to determine if the configuration would recover from such an initial angle of attack. The most forward center-of-gravity location was used in this test.

The configurations were fabricated with brass noses and with aluminum alloy or magnesium afterbodies. The noses were bored so that lead ballast could be added to shift the center of gravity between approximately 4.1 inches and 5.81 inches. Typical photographs of the experimental models are shown in figure 2.

The models were tested by firing them from the Langley 6-inch helium gum (ref. 1) located at the Langley Pilotless Aircraft Research Station at Wallops Island, Va. In operation, a model is placed in a 6-inch-diameter balsa sabot in the breach of the gun. A push plate behind the sabot bears against it and the model. A quick-opening valve admits helium to the gun barrel under about 200 pounds per square inch of pressure accelerating the sabot assembly down the 23-foot barrel to supersonic velocities. When the assembly emerges from the barrel, the three segments of the sabot and the push plate peel away, falling to earth within 50 yards. The model continues to decelerate along a ballistic trajectory during which period a continuous velocity history is obtained by means of CW Doppler velocimeter. Atmospheric conditions aloft were obtained by radiosonde measurements from an ascending balloon released at the time of the experiment. The model flight path was

NACA RM L55J13

obtained by integrating the velocity along a ballistic trajectory. The model deceleration was computed from the velocity history corrected for the effects of wind and the coefficient of drag was computed from the relationship

$$C_{D} = \frac{-W}{gqS} (a + g \sin \gamma)$$

The accuracy of the drag and Mach number measurements was within  $\pm 0.010$  and  $\pm 0.008$ , respectively.

An indication of the stability of the various configurations was obtained by firing identical models with different locations of the center of gravity. The stability of the models was assessed by inspection of the velocity histories and by comparison of the drag measurements of similar models. A smooth deceleration was taken to imply a stable, zerolift flight. Agreement of the drag measured for two identical models was additional evidence of a stable zero-lift flight. In the experiments with the 90° swept-fin configurations a marginal-stability case was determined wherein the model exhibited intermittently high and normal values of longitudinal deceleration indicating that the model was oscillating to large angles of attack.

Calculations and subsonic wind-tunnel tests indicated the neutral point of the 80° and 85° swept-fin configurations to be too far rearward for the centers of gravity to be placed there by model ballasting if the required forward locations were to be attained with the same configuration, since the range of variation of the center of gravity was limited by structural considerations. It was decided that station 5.80 (4.83 diameters from nose) represented a practicable rearmost center-of-gravity location for these configurations. Provision was made for moving the center of gravity forward by ballasting.

#### RESULTS AND DISCUSSION

#### Drag

The drag coefficients measured for the configurations tested are presented in figures 3 to 6.

Configurations having 80° sweep.- In figure 3 good agreement exists between the results for duplicate models 1-a and 1-b indicating that essentially zero-lift conditions prevailed at the time of these measurements. Model 4 (fully parabolic afterbody) exhibits unexplainably high subsonic drag; however, the drag rise of model 4 is in good agreement

with the results of reference 2. The reduced drag rise is attributable to the decreased pressure drag on the afterbody.

Configurations having 85° sweep. - In figure 4 good agreement exists between duplicate models 2-a and 2-b indicating that essentially zero-lift conditions prevailed in both flights.

Configurations having 90° sweep. - As shown in figure 5, the drag coefficients of models 3-a, 3-d, and 5 are in general agreement. The disparity in the transonic region may be due to random oscillations at transonic speeds arising from the low static margin of these models. As reported in reference 3, rounding the nose of model 5 to half the body radius gave no significant change in drag for the Mach number range investigated. The drag curve of model 6 exhibits a considerably higher level due to the additional base drag induced primarily by the annulus area behind the forebody. Drag curves for models 3-b and 3-c are not presented because their stability was too low to obtain zero-lift drag records.

Effect of fin leading-edge sweep. - As shown in figure 6, increasing the fin sweep from 80° to 85° reduced the drag of the basic configuration markedly. An additional smaller reduction was obtained by increasing the fin sweep to 90°. These drag reductions are due to reductions in wetted area and trailing-edge base area with increasing sweep.

#### Stability

As noted previously under "Experimental Configurations and Techniques," an indication of the gross stability of a configuration can be obtained from the velocity and drag histories of models which are identical except for center-of-gravity location. The results of such observations are shown in the following table. Also shown are results of low-speed (M = 0.1) wind-tunnel tests which were made by successively pivoting each configuration about vertical axes 1/4 inch apart until the point at which the model diverged was determined.

Model	λ, deg	Center-of-gravity location, percent of body length	Subsonic neutral point, percent of body length	Stability observed in free-flight test
1-a 1-b 2-a 2-b 3-a 3-b 3-c 3-d	80 80 85 85 90 90	47.1 53.6 44.8 52.2 37.9 42.5 50.9 37.9	70.2 70.2 64.6 64.6 48.0 48.0 48.0	Stable Stable Stable Stable Stable Marginal Unstable Stable
5	80 90 90	49.8 39.0 38.0	70.2 48.0 57.0	Stable Stable Stable

All models were launched at zero angle of attack except model 3-d which was launched at 100 angle of attack.

The above results show that configurations 1 and 2 were stable with the center of gravity at 54 and 52 percent of the body length, respectively. It should be noted that these are not necessarily the most rearward positions for which stability could be preserved, they are simply those center-of-gravity locations which could easily be obtained with the present models. Configuration 3 was stable with the center of gravity at 38 percent of the body length for 0° and 10° angle-of-attack launching conditions. The same configuration was marginally stable and unstable with the center of gravity at 43 and 51 percent of the body length, respectively.

#### CONCLUDING REMARKS

A series of short-span missile configurations employing  $80^{\circ}$ ,  $85^{\circ}$ , and  $90^{\circ}$  of fin leading-edge sweep have been tested in free flight. The drag was measured and an indication of stability was obtained over a Mach number range from 0.9 to 1.3 and a Reynolds number range from  $4 \times 10^{\circ}$  to  $9 \times 10^{\circ}$ . Increasing the fin sweep from  $80^{\circ}$  to  $90^{\circ}$  decreased the drag; the largest reduction occurred between  $80^{\circ}$  and  $85^{\circ}$ . The configurations having  $80^{\circ}$  and  $85^{\circ}$  of fin sweep were stable with the center of gravity as far rearward as 54 and 52 percent of the body length, respectively; the most rearward center-of-gravity location for which stability was preserved was not determined for these configurations. The configuration having  $90^{\circ}$  of leading-edge sweep was stable, marginally stable, and

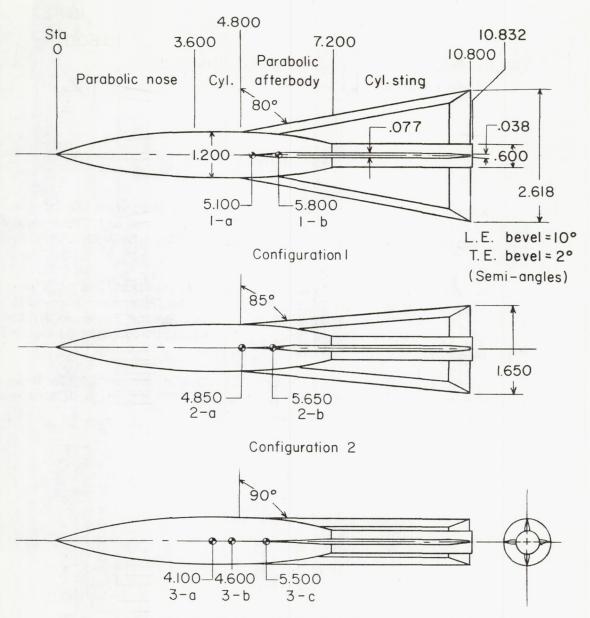
NACA RM L55J13 7

unstable with the center of gravity at 38, 43, and 51 percent of the body length, respectively.

Langley Aeronautical Laboratory,
National Advisory Committee for Aeronautics,
Langley Field, Va., October 21, 1955.

#### REFERENCES

- 1. Hall, James Rudyard: Comparison of Free-Flight Measurements of the Zero-Lift Drag Rise of Six Airplane Configurations and Their Equivalent Bodies of Revolution at Transonic Speeds. NACA RM L53J2la, 1954.
- 2. Hart, Roger G., and Katz, Ellis R.: Flight Investigations at High-Subsonic, Transonic, and Supersonic Speeds to Determine Zero-Lift Drag of Fin-Stabilized Bodies of Revolution Having Fineness Ratios of 12.5, 8.91, and 6.04 and Varying Positions of Maximum Diameter. NACA RM L9130, 1949.
- 3. Wallskog, Harvey A., and Hart, Roger G.: Investigation of the Drag of Blunt-Nosed Bodies of Revolution in Free Flight at Mach Numbers From 0.6 to 2.3. NACA RM L53D14a, 1953.

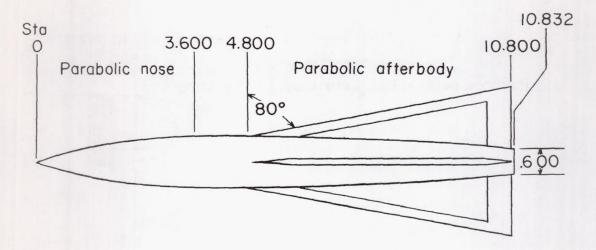


Configuration 3-d identical to 3-a, but launched at  $10^{\circ}$  angle of attack.

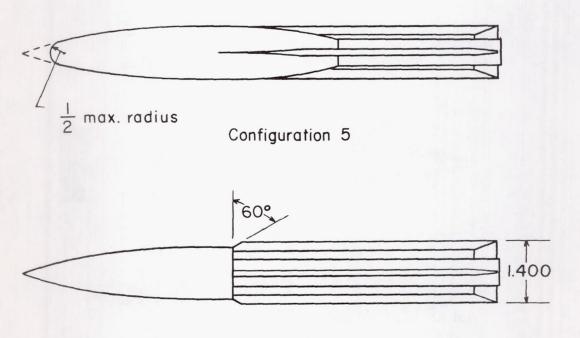
Configuration 3

#### (a) Basic configurations.

Figure 1.- Configurations tested. Symbol and letters identify location of center of gravity of models shown. All dimensions are in inches.



Configuration 4

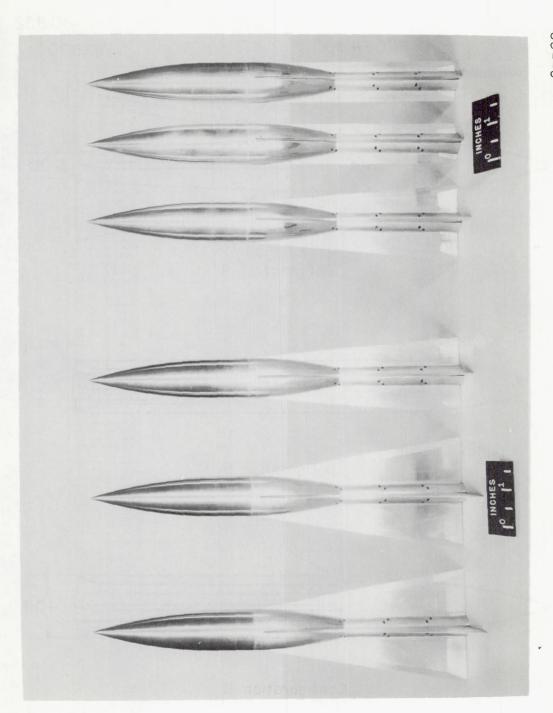


Configuration 6

(b) Modified configurations.

Figure 1.- Concluded.





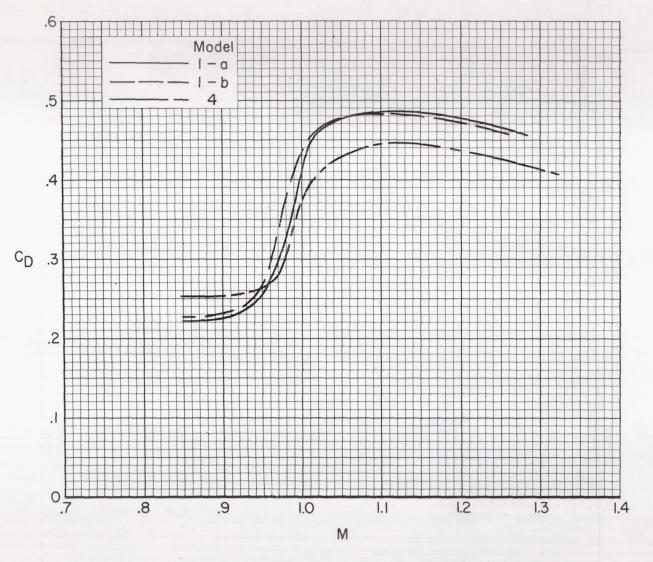


Figure 3.- Drag coefficients of models with 80° sweep angle.

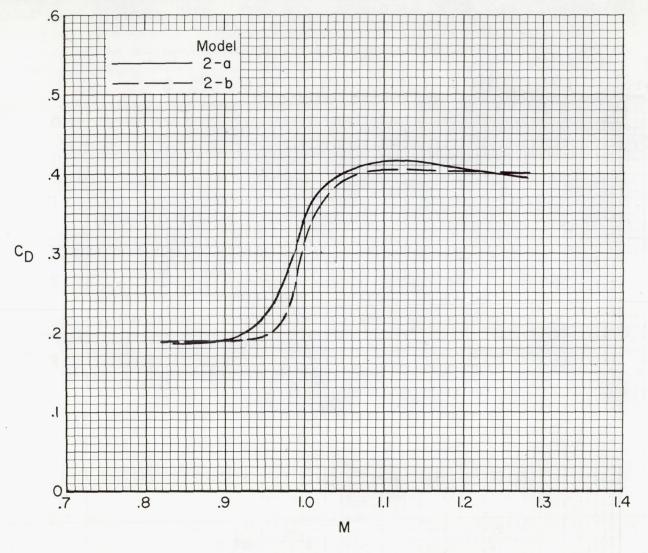


Figure 4.- Drag coefficients of models with 85° sweep angle.

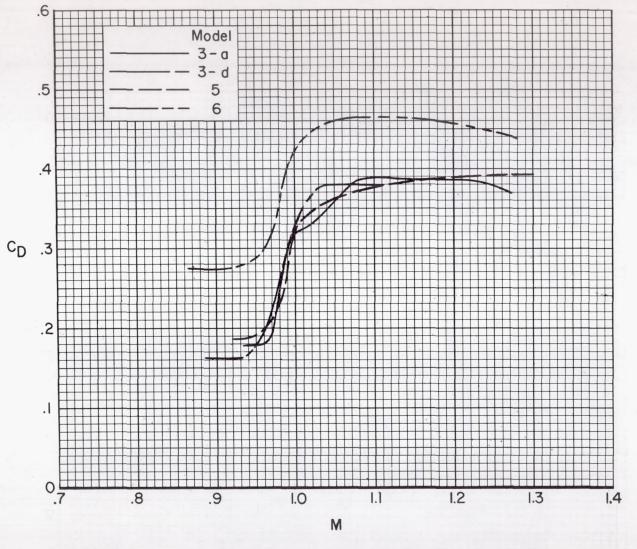


Figure 5.- Drag coefficients of models with 90° sweep angle.

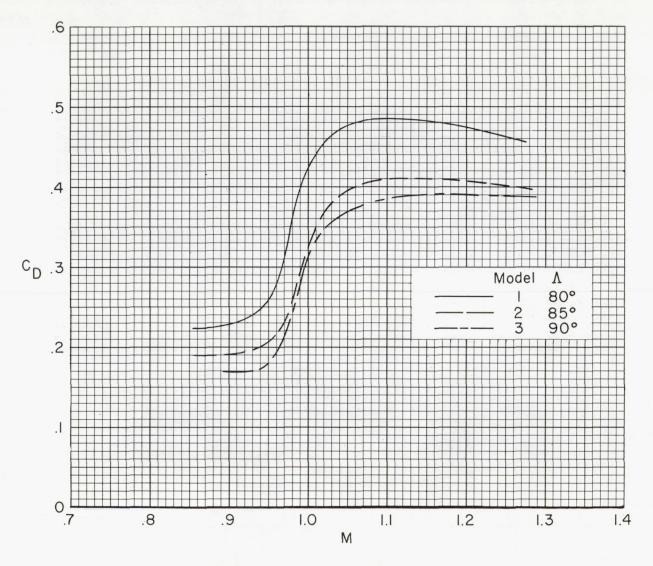


Figure 6.- Effect of wing leading-edge sweep angle on drag. Curves are averaged values for duplicate models.